

# Dynamic back analysis of structural failures in archeological sites to obtain paleo-seismic parameters using DDA

Kamai, R. and Hatzor, Y.H.

*Department of Geological and Environmental Sciences, Ben Gurion University of the Negev, Beer – Sheva, 84105, Israel.*

This paper was prepared for presentation at ICADD-7, the Seventh International Conference on Analysis of Discontinuous Deformation, held in Honolulu, Hawaii, December 10-12, 2005.

This paper was selected for presentation by a subset of the Conference Organizing Committee following review of information contained in an abstract submitted earlier by the author(s). Contents of the paper, as presented, have not been reviewed by the Conference Organizing Committee and are subject to correction by the author(s). The material, as presented, does not reflect any position of the Conference Organizing Committee. Electronic reproduction, distribution, or storage of any part of this paper for commercial purposes without the written consent of the author is prohibited.

**ABSTRACT:** The numerical Discontinuous Deformation Analysis (DDA) method was used for back analysis of structural failures in archaeological sites along the active Dead Sea rift system in Israel and preliminary constraints on historical seismic ground motions were obtained.

Two validations were first performed for calibration purposes: 1) The well studied case of a block on an inclined plane was re-studied and a much greater accuracy was obtained for the dynamic case with respect to previous publications, 2) The dynamic displacement of the foundation of a structure was simulated by inducing time-dependant displacements into the foundation block and studying the response of the overlying block.

Two case studies are presented in the paper, in which historic masonry structures were modeled and both synthetic and real earthquake records were applied as loading functions. The response of the structures was studied up to the point of incipient failure in a mechanism similar to the one observed in the field.

In both case studies the dynamic analysis was found to provide more complete and accurate results than the pseudo-static solution. Therefore, we believe that such an approach can be employed, where relevant, to provide constraints on paleo-seismic ground motions and consequently on expected PGA values in seismically active regions.

## 1. INTRODUCTION

### *1.1. Research Objectives*

In this research we present an alternative method for obtaining strong ground-motion data: by back analysis of structural failures in archaeological sites using numerical analysis by the DDA method [1]. The results of this research will provide constraints on PGA estimates, generated by the existing seismological strong motion catalogue in Israel.

In this work we focus on man-made masonry structures such as towers and arches, where hewn stones forming the building create an initial geometrical network of reference. When failure is confined to displaced blocks within an otherwise intact structure, block displacement is measurable and a mechanical analysis is possible; this can not be achieved in a completely collapsed structure. Therefore, several archaeological sites in Israel were examined for confined structural failure, and two case studies were chosen for the preliminary analysis: The Nabatean cities of Avdat and Mamshit.

## 2. VALIDATIONS

DDA Validation studies were performed for calibration purposes only, all with respect to analytical solutions. Section 2.1 repeats cases that have been validated before, yet sometimes with greater accuracy here. Section 2.2 is a new development of a validation that has never been performed before.

### 2.1. Block on an Incline

Block displacement as a function of time has been studied by many researchers, since a well known analytical solution for displacement of a point mass is readily available. The case of a single block on an incline is perhaps the most studied [2].

#### 2.1.1. Gravitation only

For a single block resting on a plane inclined at an angle  $\alpha$  with friction along the interface  $\phi$ , and subjected to gravitational acceleration  $g$ , the analytical solution for displacement  $d$  as a function of time  $t$  is given by:

$$d(t) = \frac{1}{2}at^2 = \frac{1}{2}(g \sin \alpha - g \cos \alpha \tan \phi)t^2 \quad (1)$$

The inclination of the modeled plane is  $28^\circ$  (Figure 1), and five friction angles are studied,  $\phi = 5^\circ, 10^\circ, 15^\circ, 20^\circ, 25^\circ$ . The accumulated displacements are calculated up to 1 sec.

Comparison between analytical and DDA solutions is shown in Figure 1.

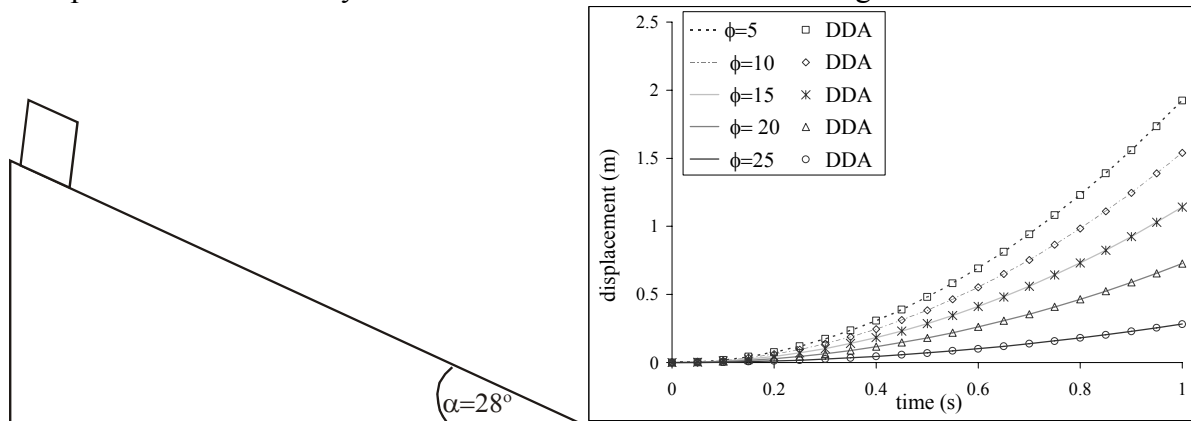


Figure 1. **A.** The model used for DDA validations of a block on an incline **B.** Block displacement – gravitational loading only. Comparison between analytical (solid line) and DDA (symbols) solutions.

#### 2.1.2. Dynamic loading

The case of a single block on an inclined plane, subjected to both gravitational load and horizontal sinusoidal acceleration, has first been examined by Hatzor and Feintuch [3] for an acceleration function consisting of a sum of up to three sines. Hatzor and Feintuch found that the accuracy of DDA prediction was within 15% of the analytical solution, provided that the numerical control parameters  $g_1, g_2$  were carefully optimized, without application of any damping<sup>(1)</sup>.

(1) Note that in the analytical solution published by Hatzor and Feintuch (2001), the resisting force during sliding for  $a_t > a_{yield}$  was neglected in the double integration.

Tsesarsky et al. [4] broadened the investigation and compared DDA results with physical results of shaking table experiments, for which an introduction of 1.5% damping was found to reduce the error significantly.

In this section, the presented validation is for an acceleration function of one sine only. The displacement  $d$  of the block at any time  $t$  is determined by double integration on the acceleration, with  $\theta$  as reference datum:

$$d = \int_{\theta}^t v = \iint_{\theta} a = g \left[ (\sin \alpha - \cos \alpha \tan \phi) (t^2 / 2 - \theta t) \right] + \frac{ag}{\omega^2} \left[ (\cos \alpha + \sin \alpha \tan \phi) (\omega \cdot \cos(\omega\theta)(t - \theta) - \sin(\omega t) + \sin(\omega\theta)) \right] \quad (2)$$

where  $\theta$  is the elapsed time from beginning of shaking until yield acceleration is reached and block motion ensues.

The model is similar to the one presented in Figure 1, but with a plane inclination of  $20^\circ$ . Three friction angles are studied:  $\phi = 20^\circ, 22^\circ, 30^\circ$ , and the accumulated displacements are computed. Figure 2.A displays the case of  $\alpha = \phi = 20^\circ$ , for which yield acceleration is zero, and displacement is calculated for more than a full cycle of the input sinusoidal earthquake. The higher friction angles,  $\phi = 22^\circ, 30^\circ$  have  $\theta = 0.089$ sec. and  $0.1802$ sec. respectively, which complicates the analytical solution after half a cycle. For that reason, the accumulated displacements in Figure 2.B for  $\phi = 22^\circ$  and  $30^\circ$  are calculated up to  $\sim 2.5$  seconds.

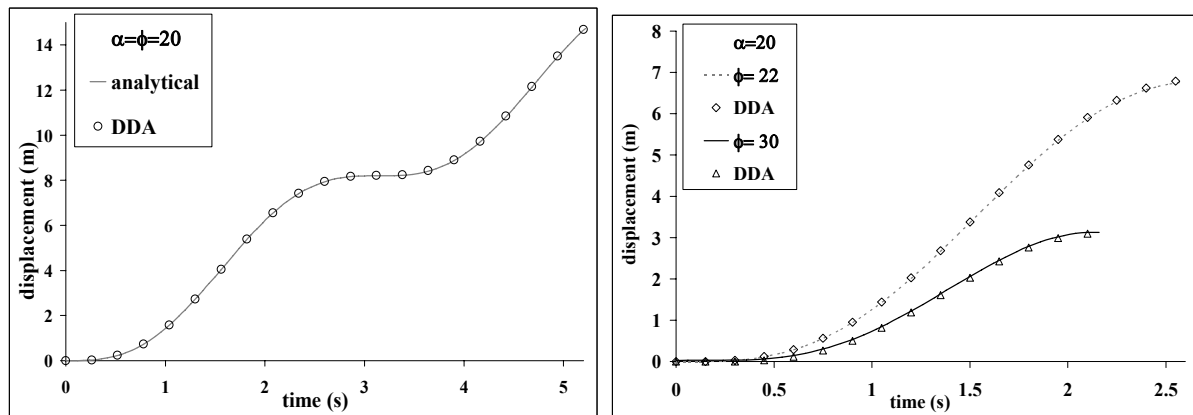


Figure 2.A. Block displacement versus time, for the case of  $\alpha = \phi = 20$ . Comparison between analytical (solid line) and DDA (symbols) solutions. **B.** Block displacement versus time, for the case of  $\alpha < \phi$ .

Figure 2.A and B. present a comparison between DDA and analytical solutions. The obtained agreement is remarkable, with maximum displacement errors ranging between 0.2% and 0.9%. The time-step size is kept constant in all DDA runs, 0.002 sec.

### 2.2. Block response to induced displacements in the foundation

DDA allows application of time-dependant displacements to “fixed” points in the mesh which are defined and positioned by the user. We use this feature to simulate seismic ground motions at the foundation and to investigate the response of a masonry structure, later in this work. We start with a validation. The purpose of this validation is to examine the accuracy of this DDA feature by comparing it to an analytical solution which is developed here for the response of a single block resting on a block which is subjected to a time-dependent displacement function. For the validation, the block system consisted of three blocks: the fixed foundation block (no.0), the induced block (no.1), and the responding block (no.2) (see Figure 3). The displacement function for block 1 was in a form of a cosine function, starting from 0:

$$d(t) = D(1 - \cos(2\pi\omega t)) \quad (3)$$

and the corresponding response of block 2 was investigated.

In order to compare between DDA and the analytical solution, the mode of failure of the analyzed block in DDA had to be constrained to sliding in one direction only without rotation or vertical motions. One way for constraining DDA to one degree of freedom in our case is by generating a block system in which block 2 has limited motion options. The block system was generated therefore such that the responding block had a very slender geometry and therefore its preferred displacement mode was one dimensional sliding with no rotation or bouncing, namely one degree of freedom, as in the analytical solution.



Figure 3. The DDA block system which constrains Block 2 to one degree of freedom – horizontal sliding only. Block 0 is the foundation block, Block 1 receives the dynamic input motion (horizontal – cyclic), and Block 2 responds.

### 2.2.1. The analytical solution

The analytical solution for this case must be computed in time steps, since the relative velocity and the direction of the force are dependant on each other. The analysis was performed by Matlab 7.0.

Figure 3 presents two blocks: The basement block (Block 0) is fixed, Block 1 is subjected to a horizontal displacement input function, and Block 2 responds dynamically.

The only force acting on Block 2 other than gravity is frictional, which immediately determines its acceleration:

$$m_2 a_2 = F_{friction} \quad (4)$$

$$\downarrow$$

$$m_2 a_2 = \mu \cdot m_2 g \quad (5)$$

$$\downarrow$$

$$a_2 = \mu \cdot g \quad (6)$$

The direction of the driving force is determined by the direction of the relative velocity between Blocks 1 and 2 ( $v_1^*$ ). When Block 1 moves to the right relative to Block 2, the frictional force pulls Block 2 in the same direction, and determines the sign of  $a_2$ .

When Block 2 is at rest in relation to Block 1, the friction force is determined by the acceleration of the Block 1 ( $a_1$ ). The threshold acceleration, under which the two blocks move in harmony, is equal to the friction coefficient multiplied by the gravitation acceleration ( $\mu g$ ). When the acceleration of Block 1 passes the threshold value, the frictional forces act in the same direction as  $a_1$ .

The positive direction is determined by the sign convention in Figure 3, and the relative velocity of Block 1 is given by:

$$v_1^* = v_1 - v_2 \tag{7}$$

The direction of the acceleration of Block 2 is set by the following boundary conditions and inequalities:

$$\begin{array}{llll}
 \text{if } v_1^* = 0 & \dots\dots\dots & \text{and } |a_1| < \mu g & \dots\dots\dots & a_2 = a_1 \\
 & & \text{and } |a_1| > \mu g & \dots\dots\dots & \text{and } a_1 > 0 & \dots\dots\dots & a_2 = \mu g \\
 & & & & \text{and } a_1 < 0 & \dots\dots\dots & a_2 = -\mu g \\
 \\
 \text{if } v_1^* \neq 0 & \dots\dots\dots & \text{and } v_1^* > 0 & \dots\dots\dots & a_2 = \mu g \\
 & & \text{and } v_1^* < 0 & \dots\dots\dots & a_2 = -\mu g
 \end{array} \tag{8}$$

2.2.2. *The numerical analysis*

A sensitivity analysis for amplitude, frequency and friction was performed. Accumulating displacement of Block 2 was calculated, and comparison between DDA and Matlab results are presented in Figure 4.

Figure 4.A presents the response of Block 2 to changing amplitudes of motion (D), with constant input frequency of 1Hz. The accumulating displacement is in direct proportion to the amplitude, as expected. Note that the three displacement curves follow the periodic behavior of the induced displacement function (T = 1 sec.), and that divergence between curves starts after 0.25 sec., where the displacement function has an inflection point.

Figure 4.B presents the response of block 2 to changing frequencies. Although the displacement amplitude is constant (2cm), the acceleration amplitude ( $A=D\omega^2$ ) increases with increasing frequency (Eq. 2). The displacement curves follow the different periods of motion, and the accumulating displacement is in direct proportion to the amplitude of the acceleration.

Figure 4.C presents the response of Block 2 to changing friction coefficients, with a constant displacement function of  $D=0.5m, f=1Hz$ . Note that the accumulating displacement is in direct proportion to the friction coefficient up to 0.5sec., where the induced displacement function changes direction. After that point the accumulating displacement of  $\mu=0.6$  is larger than  $\mu=1$ , since the high friction works in both directions: forward and backward. Note that  $\mu=0.1$  and  $\mu=0.6$  follow the periodic behavior of the displacement function, whereas  $\mu=0.6$  is in a delay of about 0.25sec.

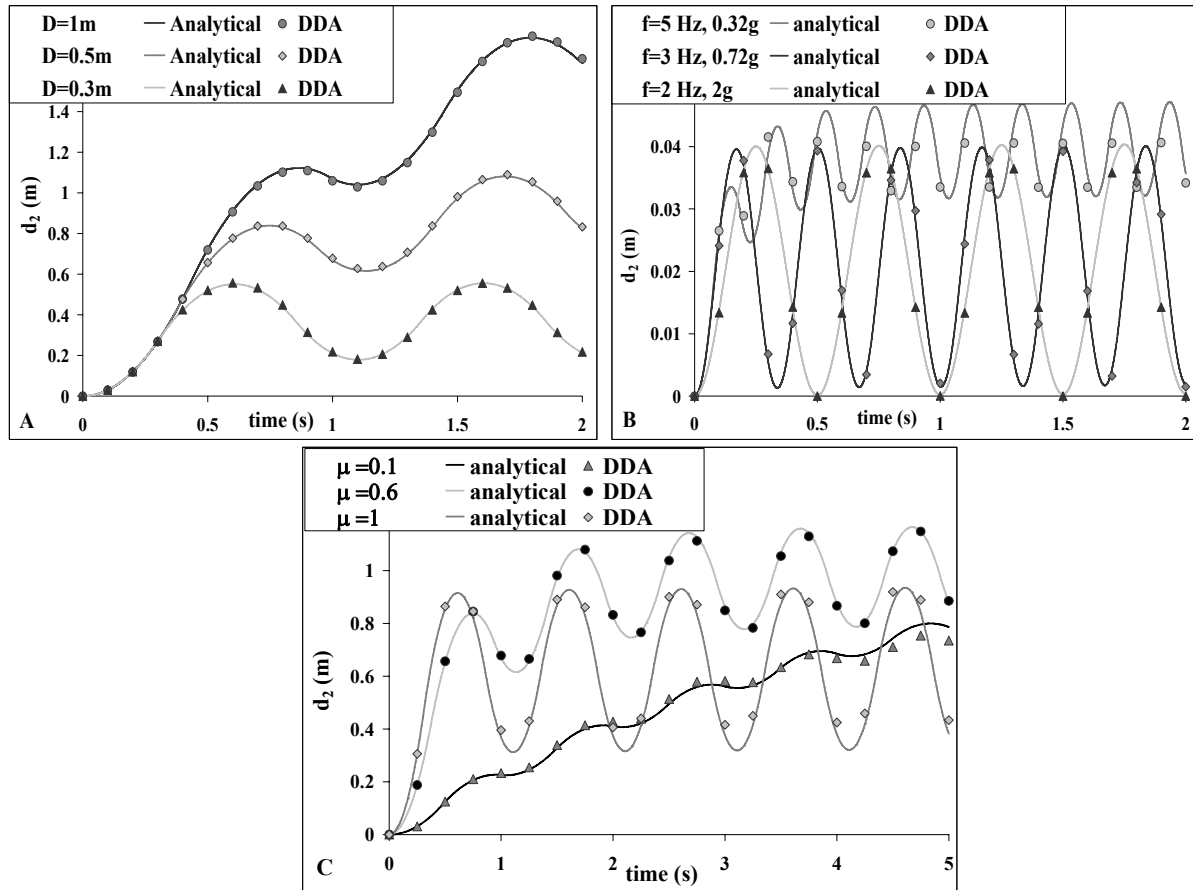


Figure 4. **A.** Response of Block 2 to displacement input of  $f=1\text{Hz}$ . Comparison between analytical (line) and DDA (symbols) solutions for different amplitudes of motion. **B.** Response of Block 2 to displacement input of  $D=0.02\text{m}$ . **C.** Response of block 2 to displacement input of  $D=0.5\text{m}$ ,  $f=1\text{Hz}$ .

A remarkable agreement can be seen in all three figures. DDA follows the analytical results in all cases, with changing friction coefficients, amplitudes, and frequencies of motion.

### 3. TWO CASE STUDIES

The applicability of dynamic DDA for back analysis of historical failures in masonry structures was tested in two archeological sites in Israel. Original building stones were sampled and transported to the Rock Mechanics Laboratory of the Negev at Ben-Gurion University. Lab tests were performed in order to obtain physical and mechanical properties of intact rock as well as block interface friction parameters. Test results are summarized in Table 1.

Table 1. Mechanical properties of original building block material.

Mechanical property	Avdat	Mamshit
Density ( $\text{Kg/m}^3$ )	2555	1890
Porosity (%)	5	30–38

Dynamic Young's modulus (GPa)	54.2	16.9
Dynamic Poisson's ratio	0.33	0.37
Dynamic Shear modulus (GPa)	20.3	6.17
Interface friction angle	35	35

3.1. Masonry Arch: results from Mamshit

A unique structural failure is noticed in a tower at the corner of the Eastern Church at the Nabatean city of Mamshit (Figure 5A), where a key stone has slid downwards out of a still standing arch (Figure 5.B). In the tower, dated back to the second half of the 4<sup>th</sup> century AD [5], the outer walls and the arched doors were built of excellent ashlar, while the interior walls were built of large squared blocks, with an occasional filling of smaller stones and earth cement (Figure 5.A) [5].



Figure 5. The damaged arch at Mamshit. **A.** The arch is embedded in a very heterogenic wall. **B.** The Keystone has slid 4cm downwards while the rest of the arch remained intact.

3.1.1. Numerical solution

Modeling the embedded arch was a challenging task because of the heterogeneity in block material shape and size (Figure 5.A). Because of material heterogeneity DDA material lines were assigned to the arch blocks in order to assign different mechanical parameters to the arch and the wall (Figure 6). Different mesh configurations and material properties were tested in order to find the conditions in which forward modeling results would fit as closely as possible the observed failure pattern in the field. The selected mesh configuration is a simple, consistent masonry wall, in which the heterogeneity is represented by lower density and stiffness than those of the hewn stones forming the arch (Figure 6).

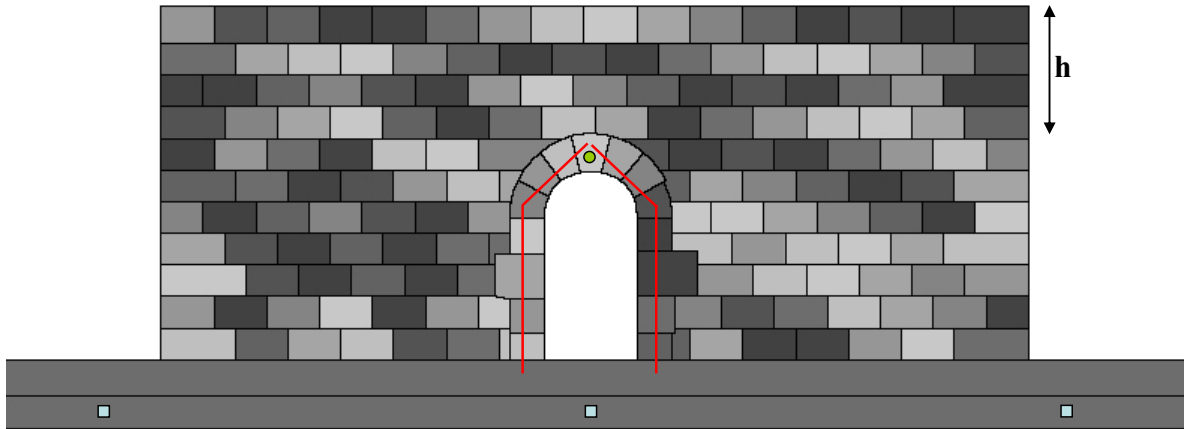


Figure 6. The final mesh configuration for the embedded arch in Mamshit. The uniform masonry wall rests on two blocks: the lower is fixed, and the overlying block can be subjected to time-dependant displacements. The height of the wall above the arch is  $h$ .

Two different loading mechanisms were examined: In the first, referred to here as ‘dis. mode’, the foundation block was subjected to time-dependant displacements, while in the second, all block centroids were subjected to time-dependant accelerations, a loading mechanism that has been studied before in DDA and is referred to as ‘qk. mode’ here.

Repeated runs of the problem revealed that the dis. mode, although validated successfully in a two-block problem, does not provide satisfactory results for a multiple block system, where over 100 blocks respond to the induced motion of a single block at the foundation.

Figures 7 and 8 display the difference in forward modeling with the dis. vs. qk. mode. In both cases the block system was loaded with a sinusoidal input function. In displacement mode the keystone undergoes upward displacement, and the entire block system is deformed, whereas in quake mode the keystone moves downwards and the rest of the mesh stays intact.

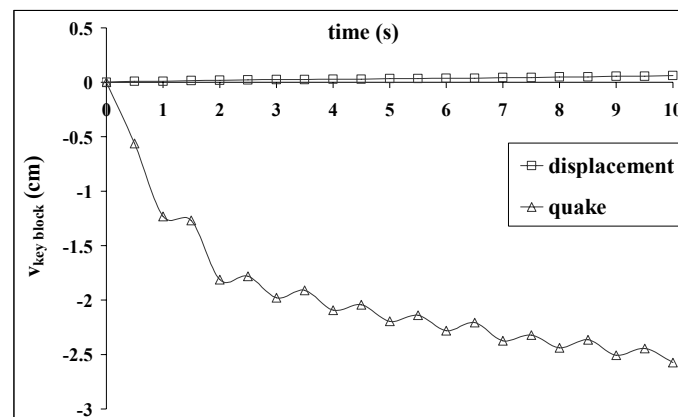


Figure 7. Influence of loading mode on keystone displacement.  $A=0.32g$  ( $D=8\text{cm}$ ),  $f=1\text{Hz}$ .

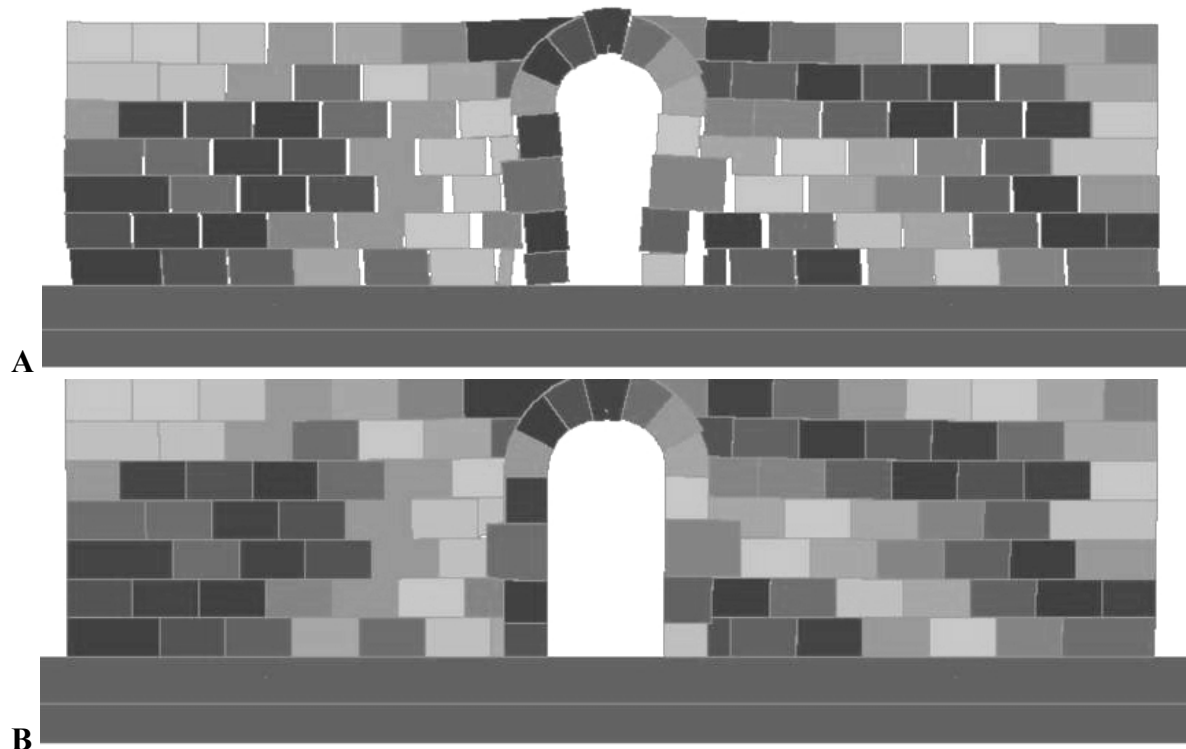


Figure 8. Response of the Mamshit block system to an earthquake with  $A=0.32g$  ( $D=8cm$ ),  $f=1Hz$ . **A.** dis. mode **B.** qk. mode.

A sensitivity analysis for the block system (Figure 6) was performed with over 50 runs. Overburden, stiffness of blocks in the structure surrounding the arch, numerical damping ( $k01$ ), and motion parameters (Amplitude and frequency) were examined. Results are presented in Figures 9 and 10, where the downward vertical displacement of the key-stone is plotted vs. time. Unless mentioned otherwise, the mechanical parameters of the block system are:  $\phi_{arch}=35$ ,  $\phi_{wall}=40$ ,  $E_{arch}=17GPa$ ,  $E_{wall}=1MPa$ ,  $h=0$ , and the analysis is performed in qk. mode. In most simulations, the input function (either acceleration or displacement) was of a sinusoidal form. A real earthquake record was used for comparison, in which the Nuweiba 1995 record, recorded in Eilat and de-convoluted to rock response (see Hatzor et al. 2004 [6] for details on this earthquake record), was scaled to different amplitudes (results are presented in Figure 10.B).

Figure 9 displays the structural response to different structural and numerical parameters. Clearly from Figure 9.A the downward displacement of the keystone became possible only after the collapse of all overlying layers, most probably due to relaxation of arching stresses. Figure 9.B implies that a difference of four orders of magnitude between the arch and wall materials is required to obtain the desired deformation, and for the deformation to be restricted to the arch only. This large difference might seem exaggerated, but a close inspection of Figure 5.A reveals the large heterogeneity and diversity of the wall, where spaces between wall-blocks are filled with soft filling materials. The soft filling materials allow for large deformations under low stresses, and drastically reduce the stiffness of the wall. We believe therefore that a 1MPa wall stiffness is reasonable.

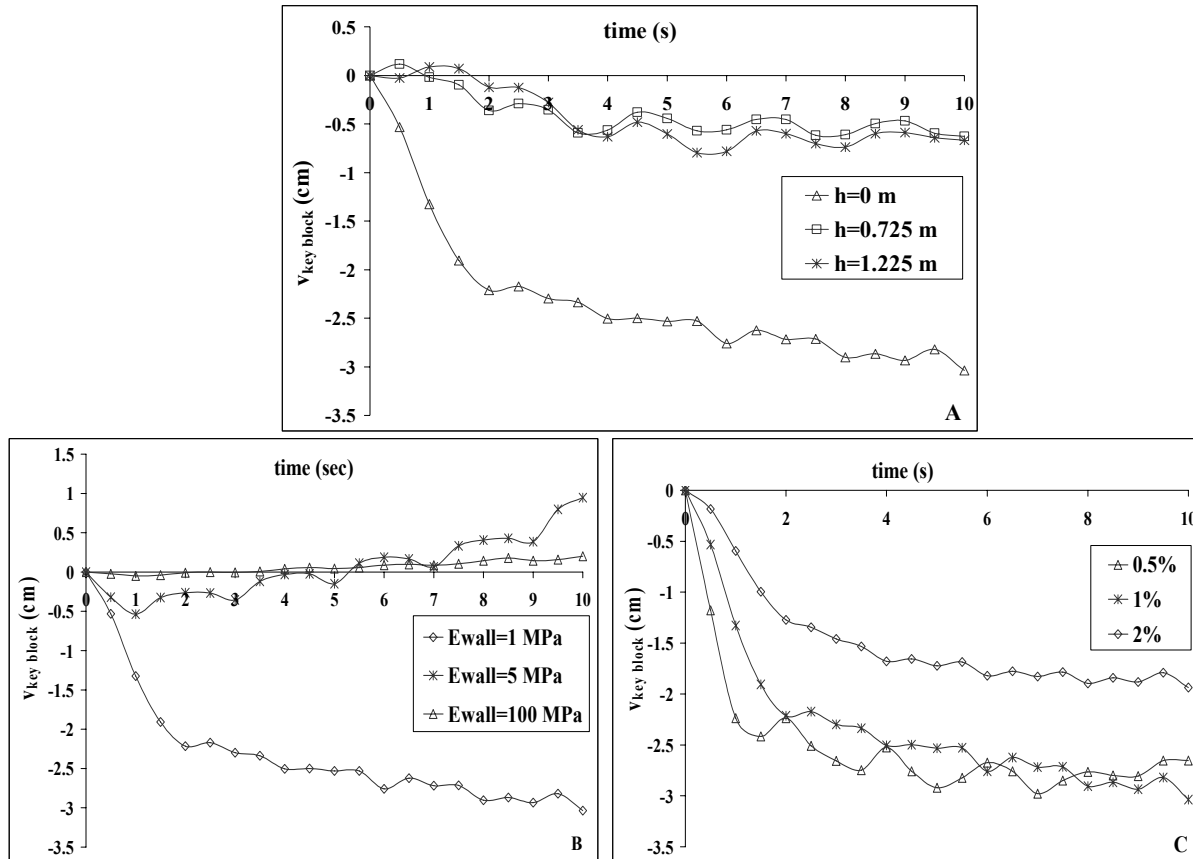


Figure 9. **A.** Influence of overburden ( $h$ ).  $A=0.5g, f=1.5Hz$ . **B.** Influence of block stiffness in surrounding wall.  $A=0.5g, f=1.5Hz$ . **C.** Influence of numerical damping ( $k_01$ ).  $A=0.5g, f=1.5Hz$ .

In Validations of simple cases where DDA results are compared with analytical solutions, the analysis should be fully dynamic ( $k_01 = 1$ ). However, it was found that in the case of a large block-system, consisting of many blocks, some energy dissipation is required for obtaining realistic results. On the basis of field and experimental studies Hatzor et al. 2004 and Tsesarsky et al. 2005 [4, 6] found that 2% velocity damping should be sufficient. Figure 9.C suggests that for the Mamshit case, the ideal amount of damping is 1%, since 2% damping reduces the displacement unnecessarily, while 0.5% damping produces stronger keystone fluctuations. When no damping is applied ( $k_01=1$ ), the analysis results in complete destruction of the structure.

Figure 10 displays the influence of input-motion parameters on keystone displacement. It can be seen from Figure 10.A that while a relatively low amplitude ( $A=0.1g$ ) results in a small displacement, a high amplitude ( $A=1g$ ) results in strong fluctuations and in a shift in the accumulated displacement direction after  $\sim 4$  sec. The best fit amplitude for this block system seems to be around 0.5g.

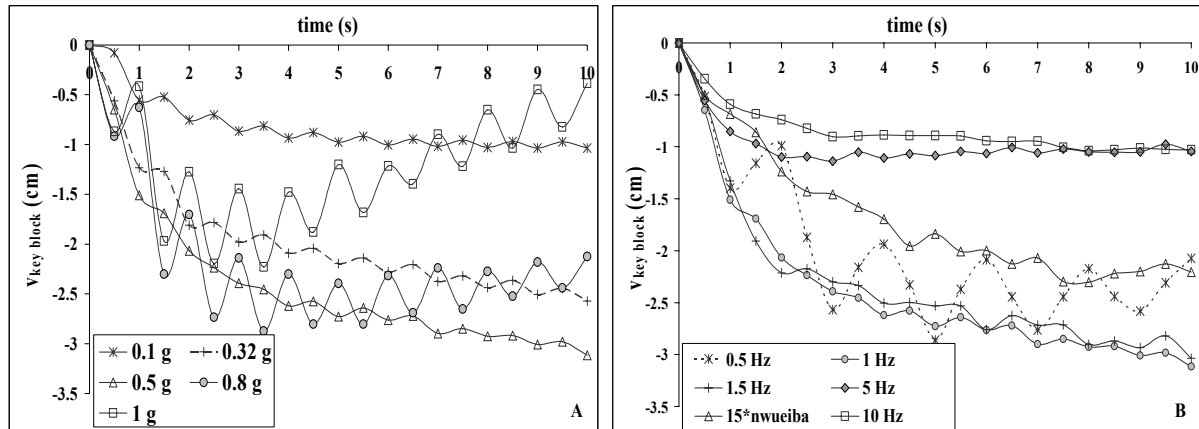


Figure 10. **A.** Influence of amplitude.  $f=1\text{Hz}$ . **B.** Influence of frequency.  $A=0.5\text{g}$ .

A very interesting behavior is displayed in Figure 10.B: the ideal frequency seems to be around 1Hz, while a low frequency (eg. 0.5Hz) results in strong fluctuations and a high frequency (eg. 5Hz and 10Hz) results in “locking” of the structure, and very little displacement. The structure response to the real Eq. record of Nuweiba 1995, amplified by 15 (PGA~0.6g) is also displayed in Figure 10.B. It can be seen that the behavior of the block system is not significantly different when a range of frequencies and additional vertical accelerations are introduced, meaning, that the results of the synthetic records are valid enough to be discussed and analyzed further.

Figure 11 displays the dynamic block system response to what we believe is the best fit earthquake, with  $A=0.5\text{g}$  and  $f=1\text{Hz}$ . The accumulating downwards displacement of the keystone is 3.11cm.

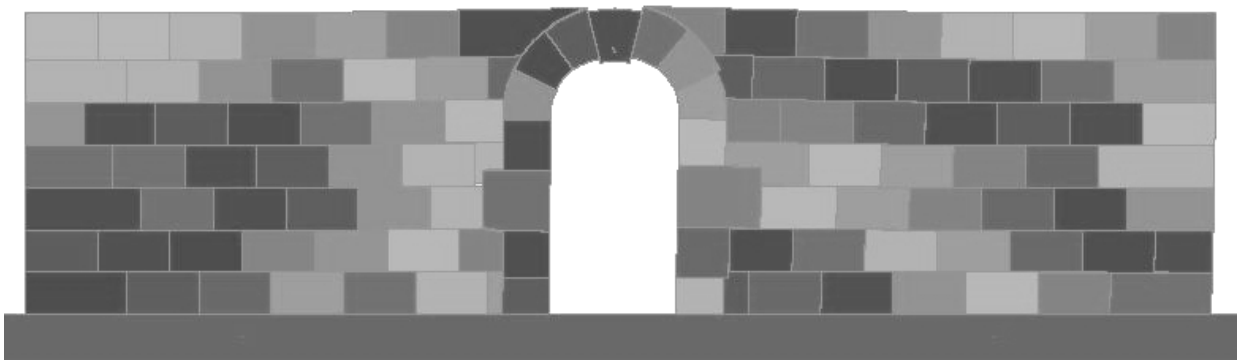


Figure 11. The result of the dynamic block system response under an earthquake with  $A=0.5\text{g}$  and  $f=1\text{Hz}$ . The accumulating downwards displacement of the keystone is 3.11cm.

### 3.2. A block on a plane: results from Avdat

Five blocks are displaced from the western wall of a Roman tower at the Nabatean city of Avdat (Figure 12). The tower, dated to 294 AD, was founded directly on bedrock, and has risen to a height of 12m, from which only 6m are left standing today [7].



Figure 12. **A.** The Roman tower in Avdat, a view of the western wall. The displaced blocks are numbered for reference. **B.** The displaced blocks.

### 3.2.1. Numerical solution

The numerical analysis of the roman tower at Avdat was performed on a block system representing the tower's northern wall, to best capture the observed westerly sliding of the three corner stones.

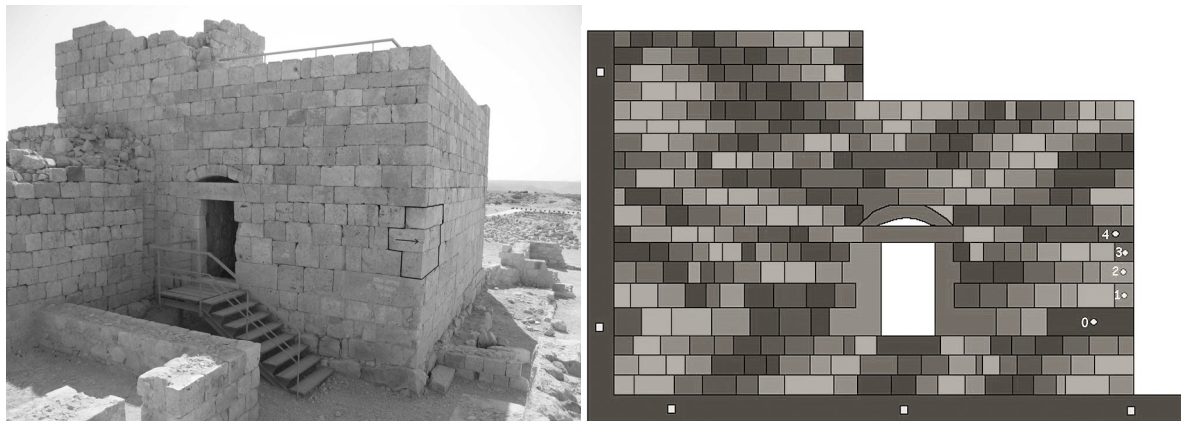


Figure 13. **A.** The northern wall of the roman tower at Avdat. The five corner blocks are marked and their displacement direction is displayed with an arrow. **B.** The DDA block system for the tower at Avdat. Five fixed points (squares) are assigned to the confining block, and five measurement points (circles) are assigned and numbered on corner blocks. 1,2 and 3 are three of the displaced blocks.

The block system, displayed in Figure 13. **B.**, was generated using program DC of DDA [1]. The DC mesh includes the entrance door and the confining block on the left side, which represents the later added structure that restricts lateral movements to the left (Figure 13. **A.**). The confining block was fixed by five fixed points, and the displacement of the five corner blocks was

measured: three of the analyzed blocks (1,2, and 3 from Figure 12.A), one above (4) and one below (0). The structure consists of one set of mechanical parameters, presented in Table 1.

The location of the displaced blocks at mid height of the wall and not at the top, where normal stresses on the frictional surfaces are at minimum, is in contradiction with the basic physical principals of a pseudo-static analysis, which would predict greater displacement of the uppermost stones. Therefore, a simulation without the confining wall was performed in order to analyze the basic behavior of the structure. The analysis predicts the exact observation that is noticed in the field, though with greater expansion, in which all blocks in the doorway level, on both sides, are displaced outwards (Figure 14).

This result might indicate arching caused by the doorway on both sides, which reduces normal stresses, and allows for block displacement in the relaxed “abutments”, in mid-height of the structure. This interesting result, again, demonstrates the extensive treatment of a dynamic solution to such a multi-block problem, versus the restricted and limited analytical approach.

A sensitivity analysis for amplitude and frequency was performed, and results are presented in Figures 15 and 16, where the average horizontal displacement ( $D_h$ ) of the five measurement points is plotted vs. time. All simulations were performed with 1% damping and a synthetic sinusoidal acceleration record.

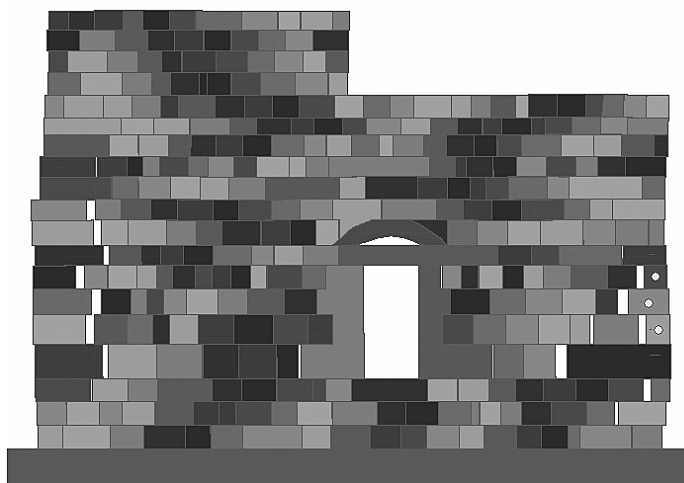


Figure 14. A simulation without a confining wall predicts the exact height of displaced blocks as is observed in the field.  $A=1.5g, f=5\text{Hz}$ .

Figure 15.A displays the influence of the amplitude on structural response, under  $f=5\text{Hz}$ . The two curves of  $A=0.8g$  and  $A=1g$  are erratic and intersect. Figure 15.B. displays the influence of frequency structural response. There is no clear trend, though it seems that displacement increases with increasing period of motion (decreasing frequency), due to longer periods of high acceleration.

Searching for the best fit set of parameters for Avdat is not as straight forward as in the previous case of the arch at Mamshit. There is no merit in comparing total block displacements since the blocks move back and forth, and do not follow a consistent trend; their total displacement depends on the duration of motion, which is unknown. Furthermore, relative displacements

between the blocks might obscure the observed total amount of displacement in the field and make the comparison meaningless.

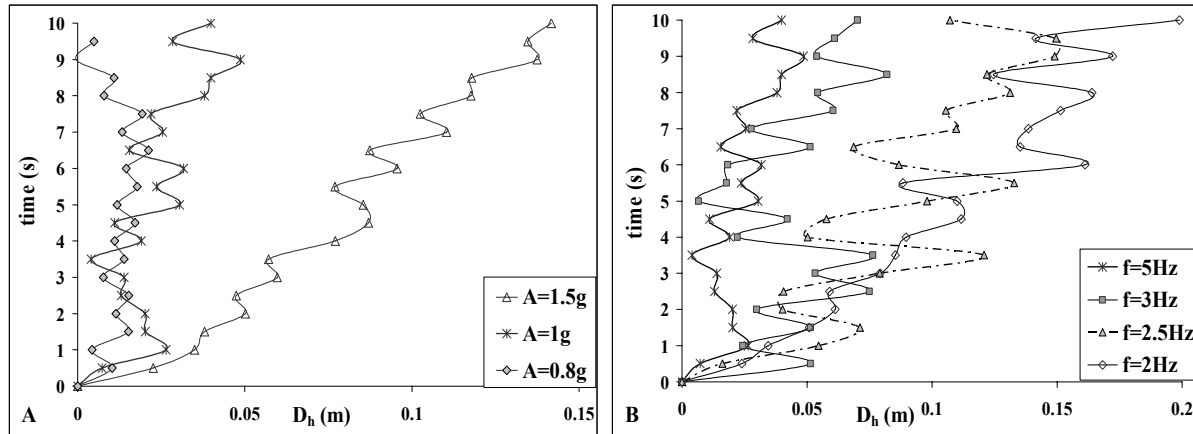


Figure 15. **A.** Influence of amplitude.  $f = 5\text{Hz}$ . **B.** Influence of frequency.  $A = 1\text{g}$ .

Figure 16.A and B display the final result of two different runs, in which only the corner blocks are displaced while the rest of the structure remains intact. Both simulations were performed with no input vertical motions ( $A_v = 0$ ). In Figure 16A the horizontal acceleration amplitude ( $A_h$ ) is  $1\text{g}$  and frequency ( $f$ ) is  $3\text{Hz}$ . The resulting horizontal displacement ( $D_{h\_avmax}$ ) is  $8\text{cm}$ . In Figure 16.B  $A_h$  is  $1.5\text{g}$ ,  $f$  is  $5\text{Hz}$ , and  $D_{h\_avmax}$  is  $14\text{cm}$ . We believe these two sets of parameters represent the best approximation that can be reached with a 2-D, numerical, back analysis of the historical earthquake that caused the observed damage in Avdat. A determination of the single, best fit set of parameters to this case study is not attempted here because of the above mentioned limitations, although the graphical output in Figure 16A better fits field measurements.

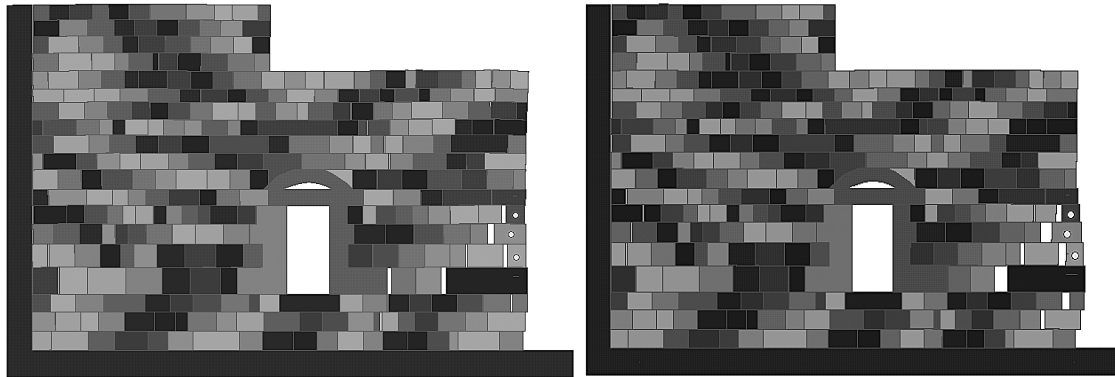


Figure 16. Best – fit simulations of the Avdat earthquake **A.**  $A_h = 1\text{g}$ ,  $A_v = 0$ ,  $f = 3\text{Hz}$ .  $D_{h\_avmax} = 8\text{cm}$ . **B.**  $A_h = 1.5\text{g}$ ,  $A_v = 0$ ,  $f = 5\text{Hz}$ .  $D_{h\_avmax} = 14\text{cm}$ .

#### 4. SUMMARY AND CONCLUSIONS

This paper describes back analysis of two earthquake induced failures in two archeological sites in the Negev, Israel, that are dated back to the 3<sup>rd</sup> and 4<sup>th</sup> centuries AD. The sites may have been subjected to more than one earthquake tremor in their history, but separation to individual seismic events is beyond the resolution or scope of this study. Back analysis is performed by subjecting the structures to simple, harmonic, dynamic loading functions and structural response is discussed in terms of displacement evolution of selected structural elements: keystone in the case of an arch (Mamshit site), and corner stones in the case of a tower (Avdat site).

##### 4.1. General conclusions

- 2D-DDA successfully duplicated structural damage that was detected and measured in the field, after the block system was generated correctly with adequate boundary conditions and material properties.
- We found that the best style of input motion for structural analysis is “quake mode” where all block centroids are loaded with time dependent acceleration simultaneously. While this loading mechanism is reasonable for a jointed rock mass, it is less adequate for masonry structures. Nevertheless, it provides a better deformation picture than simulations where the entire structure responds to an input displacement at the foundation block (“displacement mode”).
- Clearly, application of “quake” mode does not allow for wave propagation phenomena such as amplification, de-amplification, etc. to take place when the motion is transferred from bedrock to the structure. Further research is required to resolve the significance of rock-structure interaction processes when masonry structures are founded on stiff rock, for forward numerical modeling.
- As a result of applying “quake” mode and a harmonic sinusoidal function the obtained ground-motion parameters may be higher than reasonably expected (eg. 1g at Avdat). Therefore, we do not argue at this stage for exact historical ground motion restoration, but focus on the structural behavior and failure patterns that are obtained, and compare them to field observations.
- The sensitivity analysis performed with DDA demonstrates the importance of the dynamic structural response, thus stressing the role of the duration and frequency of ground motion. This is a strong proof for the partial determination of motion by the value of PGA, often used in the fields of seismic hazard assessment and design.
- We wish to emphasize that over-all structure response is as important as local displacement measurements. Therefore, graphical output of the deformed mesh configuration is as valuable as the quantitative measurement point data, since it enables us to understand the evolution of the structural damage and the dominant failure modes.

##### 4.2. Back analysis of masonry arch (Mamshit)

- We found that downward displacement of the keystone was only possible after the collapse of overlying layers. A process that must have caused relaxation of arching stresses.
- We found that most damage resulted from horizontal motions and that the significance of vertical motions was negligible.

- We found that most of the accumulated keystone displacement took place in the first two seconds of the motion; therefore much longer runs are not necessary. This result may also suggest the duration of the earthquake that caused the detected damage.
- Our best estimate for the horizontal amplitude and frequency of the earthquake that caused the damage in Mamshit is 0.5g, and 1 Hz respectively. Resolution of the date and number of events is beyond the scope of this paper.

#### 4.3. Back analysis of masonry tower (Avdat)

- 2D analysis of corner stones in the tower ignores in plane rotations, which may play a significant role in the dynamic deformation of the structure.
- A very unique structural failure in Avdat, in which mid-height blocks have been laterally displaced, is duplicated perfectly by dynamic DDA. The results provide an insight into the structural dynamic behavior, which could not have been achieved by a different analysis approach, certainly not by a pseudo-static approach.
- We found two possible sets of dynamic input motion that could have generated the observed failure in the field: A)  $A_h = 1g, f = 3\text{Hz}$ ; B)  $A_h = 1.5g, f = 1.5\text{Hz}$ . The best fit set of parameters is not determined conclusively since a meaningful and finite comparison measure such as total block displacement will not portray the failure mechanism properly, as blocks move back and forth, sometimes with no obvious trend, and so total displacement is a matter of time frame.

## 5. ACKNOWLEDGMENTS

Dr. Gen-hua Shi is thanked for providing us with his latest version of DDA (2003). Dr. Zvika Zuk from Israel Nature and Parks Authority and Dr. Tali Gini of Israel Authority of Antiquities are thanked for supervising block sampling and measurements in the field. Finally, Dr. Shmulik Marco of Tel Aviv University is thanked for joint field trips and stimulating discussions.

## 6. REFERENCES

- (1) Shi, G.-H. 1993. *Block System Modeling by Discontinuous Deformation Analysis*. Southhampton, UK: Computational Mechanics Publication.
- (2) MacLaughlin, M.M. and D.M. Doolin. 2005. Review of validation of the Discontinuous Deformation Analysis (DDA) method. *Int. J. Numer. Anal. Meth. Geomech.* 29:
- (3) Hatzor, Y.H. and A. Feintuch. 2001. The validity of dynamic block displacement prediction using DDA. *Int. J. Rock Mech. Min. Sci.* 38: 599-606.
- (4) Tsesarsky, M., Y.H. Hatzor and N. Sitar. 2005. Dynamic displacement of a block on an inclined plane: Analytical, experimental and DDA results. Technical note. *Rock Mechanics and Rock Engineering.* 38: 2,153-167.
- (5) Negev, A. 1988. The Architecture of Mamshit. *Quedem. monographs of the institute of archaeology.* ed.
- (6) Hatzor, Y.H., A.A. Arzi, Y. Zaslavsky and A. Shapira. 2004. Dynamic stability analysis of jointed rock slopes using the DDA method: King Herod's Palace, Masada, Israel. *Int. J. Rock Mech. Min. Sci.* (in press):
- (7) Negev, A. 1997. The Architecture of Oboda. *Quedem. monographs of the institute of archaeology.* ed.